Some Aspects of the Metal–Insulator Transition

Jeremy K. Burdett
Department of Chemistry and The James Franck Institute, The University of Chicago, Chicago, IL 60637, U.S.A.

1 Introduction

Studies of metals and semiconductors *per se* have been important endeavours for the physics community for many years, but one of the most interesting areas from both chemical and physical points of view is identification of the factors determining whether a particular solid is a conductor of electricity, how well it does it, and how external events such as pressure and temperature may move a system from one régime to the other. From the viewpoint of the electronic structure of the solid, a metal is simply a system with a partially-filled energy band. But what are the rules associated with the generation of this state of affairs, and what are the factors which compete with them and which lead to insulators? Certainly the predictive capabilities of existing ideas are not particularly good. Witness, for example, the surprise associated with the unravelling of the properties of the high-temperature superconductors and the difficulty in finding good models with which to describe them. Indeed, one of the consequences of the discovery of this series of superconducting copper and bismuth oxides has been the resurfacing of many old, unsolved, problems in this area. This review will try to set out some of the central electronic considerations in this field and highlight some of them with examples in more detail.

2 The 'Metallic' Bond

2.1 Two Types of Electronic Description

The question of metals and insulators (the 'dynamic' electron problem) makes immediate contact with the way that the electronic structure of solids (the 'static' electron problem) is described. Like many chemical problems the nub of some of the theoretical considerations may be phrased in terms of a balance between the one-electron and two-electron terms in the Hamiltonian and so are frequently difficult to quantify. The simplest approach starts with the bonding situation in the H_2 molecule using the molecular orbital or Mulliken–Hund model.[1] In-phase and out-of-phase combinations of the two 1*s* orbitals (ϕ_1,ϕ_2) lead to bonding and antibonding combinations (ψ_b,ψ_a). The simplest wave function for the $(\psi_b)^2$ configuration is

$$\Psi_{MH} = \psi_b(1)\psi_b(2) \quad (1)$$
$$= \tfrac{1}{2}(\phi_1 + \phi_2)(1)(\phi_1 + \phi_2)(2)$$
$$= \tfrac{1}{2}[\phi_1(1)\phi_1(2) + \phi_2(1)\phi_2(2) + \phi_1(1)\phi_2(2) + \phi_2(1)\phi_1(2)]$$

with a total electronic energy of

$$E_T = 2(\alpha + \beta) + U/2 \quad (2)$$

Here $\alpha = \langle\phi_i|\mathscr{H}^{eff}|\phi_i\rangle$ and β the interaction integral $= \langle\phi_i|\mathscr{H}^{eff}|\phi_j\rangle$, using the Hückel approach. $\mathscr{H}^{eff}$ is some effective Hamilitonian for the problem. $U = \langle\phi_i(1)\phi_i(2)\, r_{12}^{-1}|\phi_i(1)\phi_i(2)\rangle$, a two-electron term, is the Coulombic repulsion between two electrons located in the same orbital on the same atom. Since there is a finite probability from the wavefunction of equation 1 that the two electrons can reside simultaneously on the same atom its contribution to the energy of equation 2 is non-zero. The energy of the ground state is thus the sum of the two types of terms, those which depend on just one electron (α,β) and are negative, and that which depends on two electrons (U) and is positive. The wavefunction of equation 1 describes an arrangement where the two electrons are delocalized *via* the MO description over the two hydrogen atoms.

A different approach is used when the two hydrogen atoms are far apart. The chance that both electrons can reside on the same atom together is small and thus inclusion of terms such as $\phi_1(1)\phi_1(2)$ inappropriate. Instead a Heitler–London wavefunction is written as

$$\Psi_{HL} = 1/\sqrt{2}[\phi_1(1)\phi_2(2) + \phi_1(2)\phi_2(1)] \quad (3)$$

The electrons are now localized, one on each of the hydrogen atoms (H·H·). The energy of this state is just $E_T = 2\alpha$. Two higher energy states where both electrons are forced to lie on the same atom as in H^+H^- and H^-H^+.

$$\Psi'_{HL} = \phi_1(1)\phi_1(2) \text{ and } \Psi''_{HL} = \phi_2(1)\phi_2(2) \quad (4)$$

have an energy of $E_T = 2\alpha + U$.

The energy difference between delocalized and localized descriptions[2] is determined by the critical ratio $\kappa = U/4\beta$. If $\kappa \gg 1$ the localized description is appropriate, but if $\kappa \gg 1$ the localized picture is the one to use. κ measures the importance of one-electron (β) and two-electron (U) contributions to the energy. Many observations in chemistry are of the same type. The value of P/Δ, where P is the pairing energy and Δ the t_{2g}/e_g splitting (respectively two- and one-electron terms), discriminates between high-spin and low-spin complexes of the transition metals.

These simple ideas may be extended to solids. If the interactions (β) between orbitals on adjacent atoms are small compared to the on-site repulsion (U) then the localized Heitler–London description is appropriate. This is the case for example, for the copper $x^2 - y^2$ electrons in La_2CuO_4. The result is a semiconductor with an activation energy for electron movement, the Coulombic penalty associated with placing two electrons on the same atom at the same time. If β is large compared to the on-site repulsion U, then the Mulliken–Hund description is the one to use. Determination of the magnitude of the parameter κ is not a simple task however.

2.2 Localized and Delocalized Bonding

The pair of words 'delocalized' and its antonym 'localized' have a variety of meanings within the chemical literature and so one should be careful with their use. In the previous section we have used the terms to describe Mulliken–Hund and Heitler–London functions respectively, in accord with the types of terms appearing in the wavefunctions of equations 1 and 3. In a separate but related usage, the bonding in metals is frequently described as

Jeremy Burdett was born in London and was educated at Magdalene College Cambridge and The University of Michigan. He obtained his Ph.D. from Cambridge in 1972 with J. J. Turner. He has been on the faculty of The University of Chicago since 1978 and is presently Professor and Chairman. His interests are in physical aspects of inorganic chemistry, especially structural –electronic relationships in molecules and solids. He is the author of some 200 articles and 4 books.

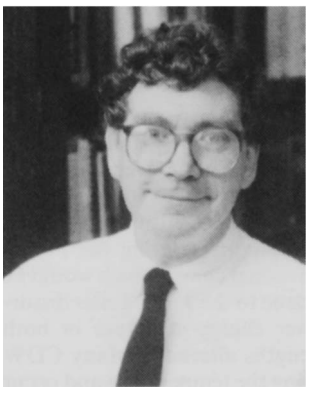

delocalized since these materials are electrical conductors and therefore contain itinerant electrons By way of contrast the bonding in insulators is often described as localized since the electrons are not itinerant Although one should be much stricter in the choice of language, since current usage is so ingrained it is difficult to be Included in the very broad spectrum of systems for which the Mulliken–Hund or molecular orbital picture is appropriate are both the σ and π manifolds of organic systems, including the classic Huckel 'delocalized' picture for the π systems of conjugated molecules The photoelectron spectra of such compounds are well-matched by simple molecular orbital constructs However, the σ manifold of these molecules is usually described as being made up of 'localized' two-centre, two-electron bonds Well-described too by the Mulliken–Hund approach are, not only materials such as diamond and Zintl phases, but also those of metalloids such as bismuth The link between the two, apparently contradictory, theoretical pictures is well-known,[3] but definitely worth repeating here If in a molecule there is a set of N bonding orbitals each occupied by an electron pair, and there are N close contacts in the structure, then by taking judiciously chosen linear combinations of the delocalized orbitals a set of N localized two-electron, two-centre bonds may frequently be generated – the bond orbitals As long as one is discussing 'collective' properties[3] of the electrons, such as total energy or electron density, then either the molecular orbital or bond orbital approach is valid Non-collective properties such as photoelectron spectra require the use of the molecular orbital delocalized model In methane four equivalent, 'localized' C–H 'bonds' may be generated from the set of four filled ($a_1 + t_2$) orbitals but the photoelectron spectrum shows two peaks If there are insufficient pairs of electrons for such bonds, as in the π manifold of benzene (three bonding π pairs but six close contacts), then such a transformation is not possible A circle drawn inside the hexagon describes this state of affairs Thus both s and p manifolds may be described by the molecular orbital method (this has to be used in the interpretation of photoelectron spectra) but the delocalized orbitals may be 'localized' in one case (σ) but not in the other (π) to give two-centre, two-electron bonds

An analogous picture holds for solids For diamond the energy bands created *via* the delocalized picture may be localized in the same way as for methane by the construction of Wannier functions [4] However, here there is a very important restriction In order to do this, the energy band must be filled with electrons Thus for quartz, SiO_2, the result is a localized picture with the two-centre, two-electron bonds between silicon and oxygen, as found in the Lewis structure However, for the band structure which describes the π manifold of graphite, just as in benzene, such a transformation is not possible since the band is half-filled The delocalized picture has to be used

The most important point of this discussion is that the option of an electronic description in terms of localized orbitals is available only for a subset of Mulliken–Hund systems, namely those with a filled band or with the right number of filled orbitals in a molecule The delocalized picture is, however, always appropriate for all Mulliken–Hund systems Recognition of this fact has led in the molecular realm to dramatic progress in recent years in the electronic descriptions[5] of a wide range of compounds, including cage, cluster, and organometallic examples Thus the view of the 'metallic bond' in solids we would like to stress is that it corresponds to a Mulliken–Hund description of the solid, but without the option of the construction of localized Wannier functions Since the construction of such functions require the presence of a filled band of electrons, a metal corresponds to the presence of a partially filled energy band Thus there is no special type of chemical bonding associated with the 'metallic' bond The band itself is generated by orbital overlap between adjacent atoms just as for the molecular orbitals of methane Probably the term 'metallic bond' should be dropped from the literature The challenge for the chemist is to identify the factors which lead to partially filled bands of this type for some systems and not for others

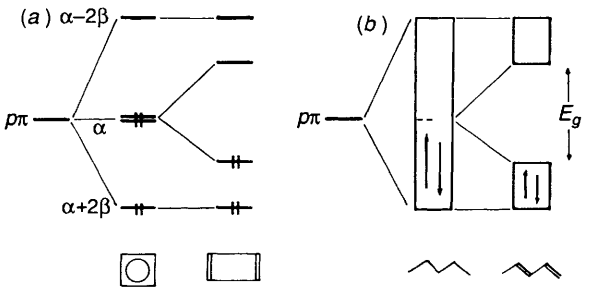

Figure 1 The relationship between (a) the Jahn Teller distortion in cyclobutadiene and (b) the Peierls distortion of a polyacetylene chain

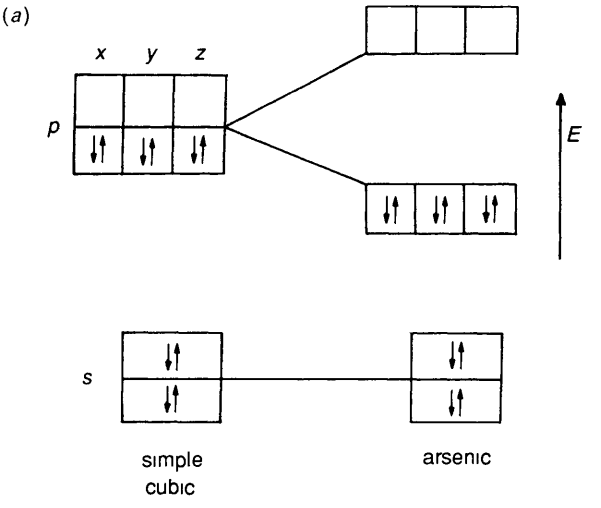

Figure 2 (a) The three-dimensional Peierls distortion of the simple cubic structure for the Group 15 elements to give (b) the structures of arsenic and black phosphorus (The simplest derivative structures are also shown)

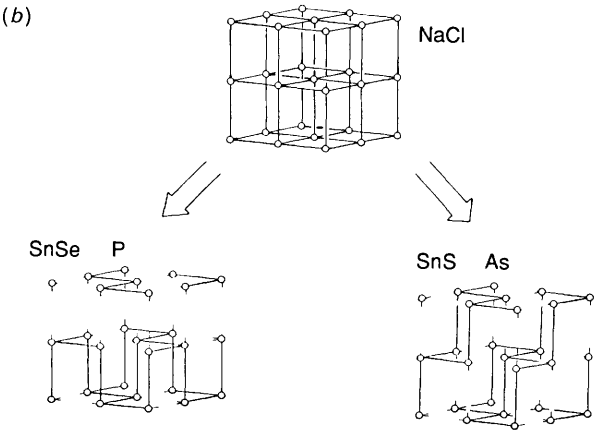

2.3 CDW and Peierls Distortions

By analogy with Jahn–Teller ideas in molecules, partially-filled energy bands are in principle subject to geometrical distortions associated with a lowering of the total energy and variously described as Fermi surface instabilities, Charge Density Waves (CDW), or Peierls distortions As the structure changes a gap may open at the Fermi level to create an insulator or semiconductor [6] Figure 1 shows a classic picture relating the Peierls distortion of the infinite one-dimensional chain (which would be metallic if half-filled) of polyacetylene to the Jahn–Teller distortion of cyclobutadiene The lower energy structure in both systems is one where the bond lengths alternate Many CDW instabilities are triggered by lowering the temperature and occur in a range of systems which cover a wide range of chemical types

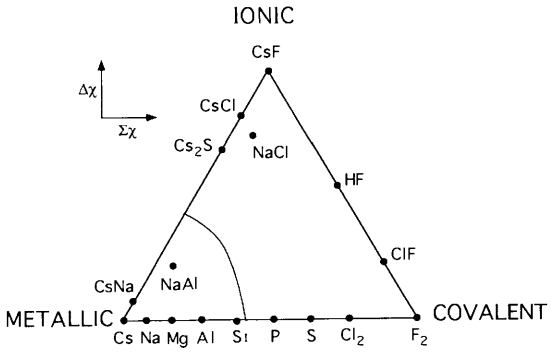

Figure 3 A van Arkel Ketelaar diagram used to separate metallic ionic and covalent bonding in solids The indices used here are the sum and difference of the atomic electronegativities

metal oxides and sulfides, molecular metals, and the elements themselves The three-dimensional analogue of Figure 1a shown in Figure 2a is the description[7] of the structures (Figure 2b) of the Group 15 elements in terms of three-dimensional Peierls distortions of the simple cubic structure The latter with its half-filled collection of p orbitals would be a metal As a result of the distortion from cubic phosphorus the coordination number is reduced from six to three, no energy bands are partially filled, and the three 'sp^3' bonds and lone pair of the localized model are able to be generated In this case the distortion may be reversed by pressure Under these conditions black phosphorus becomes a metal In an exactly analogous way hydrogen is predicted to become a metal under (4 Mbar or higher) pressure Thus in addition to the criterion for the generation of a metal of a partially filled energy band is the importance of CDW distortions which will open a gap and enable a localized picture to be drawn Peierls argued that in one-dimension a gap would always be opened on distortion (as in Figure 1a), but that this was generally not the case in two or three dimensions The details are beyond the scope of this review and we refer the reader elsewhere[6] for a fuller discussion

The variation in the magnitude of the driving force from system to system is thus a crucial parameter to understand Figure 3 shows an interesting result, namely a van Arkel–Ketelaar diagram used traditionally to separate compounds into 'covalent' 'ionic', and 'metallic' regions In view of the discussion above, horizontal excursions across the diagram, from 'metallic' to 'covalent', are concerned with the variation in the magnitude of this driving force These diagrams may be constructed quantitatively[8] using as a horizontal coordinate the sum of the electronegativities (from configurationally averaged ionization energies) of the constituents, and as a vertical axis their difference Obviously the electronegativity difference is a good measure of ionic character, but why does the electronegativity sum lead to a good separation?

First it should be recognized that the Peierls distortion is driven by the energetic preferences (Figure 1a) of the occupied energy levels which lie at highest energy Resisting the distortion, driven by these electrons, are both the 'elastic' forces of the underlying electronic structure and the repulsive part of the interatomic potential There are some simple considerations which show why elemental lithium has a close-packed structure and is a metal, but elemental fluorine is an insulator and is composed of F_2 dimers Calculations show[9] a dramatic increase in the driving force for the distortion on moving from left to right across the diagram Although there are several ingredients, the part of the electronic picture which is easiest to see is that associated with the orbital interaction integrals which link adjacent atoms β in the Huckel language Using the Wolfsberg–Helmholz approximation these are written as being directly proportional to the sum of the corresponding α values Since these increase smoothly in magnitude on moving from left to right across the periodic table an increase in the magnitude of the distortion energy, and thus the distortion itself, should be expected from this source The α values used in calculations of this type come from atomic spectral data, and so it is particularly interesting to see that the horizontal index for the van Arkel–Ketelaar diagram of Figure 3 is just the sum of the atomic electronegatives evaluated from the same atomic data

2.4 The 'Metallic' Bond

The discussion above emphasizes the need to remove from the vernacular the traditional idea that the metallic bond represents a different bonding type Metals of the type described above are just those systems, usually well-described by the orbital model, but where the driving force is not large enough to open a gap at the Fermi level An area where the traditional view of the metallic bond is especially inappropriate is that of the molecular metals, exemplified most recently by the doped fullerenes These are simply systems, held together by van der Waals forces, where there is a small, but important overlap between the orbitals of each unit to form energy bands On doping by either intrinsic or extrinsic means, these bands may become partially filled and metallic conduction possible The electronic description of these materials is readily accessible by tight-binding calculations, the solid-state analogue of the molecular orbital approach Although outside the scope of this review, for a wide range of solids the correlation between theory using this orbital model and experiment (see for example reference 6) in terms of the identification of the $\boldsymbol{k}$ vectors which nest the Fermi surface with those observed from diffuse X-ray scattering experiments is impressive

3 Metals and Insulators

3.1 Two Broad Classes of Metal–Insulator Transitions

The metal–insulator transition is a many-faceted phenomenon, but let us try to paint a picture which may be an oversimplification but will enable a broad overview In the previous section two routes to the generation of an insulator were outlined The first was one where the on-site Coulomb repulsion is so large that the electronic description of the system required the use of a Heitler–London wavefunction of the localized type Electrical conduction is activated, the activation energy being associated with the accommodation of two electrons lying simultaneously in the same atomic orbital and thus subject to a strong Coulombic repulsion between them The second route led to an insulator by the filling of the highest occupied energy band Conduction may only now occur by excitation of electrons to the valence band which may not occur at ambient temperatures Because the band is filled, localized Wannier functions may be constructed for the system Sometimes, as in diamond, these localized functions look just like the ones expected from simple chemical considerations In MoS_2, however, the 'localized' function[10] is 'delocalized' over three atomic centres just like the bonding orbital in the H_3^+ molecule Thus there is, using the term 'localized' in somewhat different ways, a correspondence between insulating behaviour and 'localized' bonding

Figure 4 shows these two broad classes of metal–insulator transitions and how, for the half-filled band, an insulator may be generated either by localization or *via* a CDW distortion

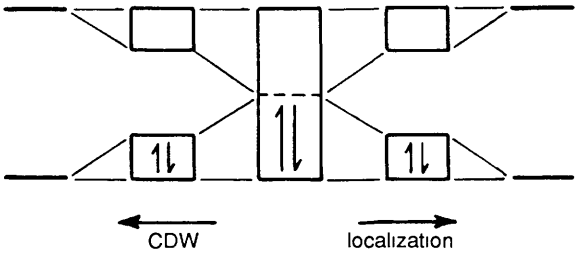

Figure 4 How an insulator may be generated either by localization or *via* a CDW distortion for the half-filled band

Elemental hydrogen provides example of all three types Under high pressure, hydrogen becomes a metal, this corresponds to the picture in the centre of the figure Under ordinary pressures hydrogen exists as dimers, regarded as being generated from the metallic structure *via* a CDW distortion at left The situation at the right describes the electronic picture for hydrogen *atoms* at large internuclear distances

Mott suggested that systems where transitions from insulator to metal occur as the particle density increases may be regarded in terms of a screened Coulomb potential between the conduction electrons and the nuclei There is a critical screening constant,[11] determined by the electron density, at which the electrons condense around the nuclei to give an insulator An example here might be the metal–insulator transition associated with the increase in density of electrons of solutions of sodium in liquid ammonia Dilute solutions are blue ('localized' solvated electrons), but more concentrated ones bronze and metallic The transition between the two is set by the concentration of sodium Similar considerations are probably behind the generation of metallic (and superconducting) $La_{2-x}Sr_xCuO_4$ for $x > 0.05$ by doping the insulator ($x = 0$) with strontium Here the dopant is 'holes' in contrast to the electrons of the sodium/liquid ammonia case The first holes which are introduced by doping are trapped at local sites by a local distortion, the small polaron The idea, suggested by Hubbard,[11] of competition between interatomic overlap leading to band formation and the localization of electrons when the on-site Coulomb repulsion (U) is high has been described earlier On this model the critical ratio determining the metal-antiferromagnetic insulator transition for the half-filled band is U/W, a parameter related to κ, where W is the band width The two bands in the antiferromagnetic insulator are separated by a Hubbard or correlation gap The lower level at the far right of Figure 4 is best described by equation 3 and the upper level by equation 4 Thus the energy gap between them, the Hubbard U, is simply the sum of the ionization potential and electron affinity of the separated atoms Evaluation of U for solids is not quite as simple [1] Insulators of this type are frequently called Mott–Hubbard insulators Anderson[11] developed a model where disorder leads to a mobility edge within the band of the ordered metal which separates localized and delocalized states Since disorder is invariably introduced by doping (*e g* , in $La_{2-x}Sr_xCuO_4$) separation of the Mott, Hubbard, and Anderson aspects of the transition are difficult Of particular concern at present is how, in detail, doping an antiferromagnetic insulator leads to a metal

3.2 The Rôle of Band Overlap

If filled bands give rise to insulators and partially-filled bands to metals, then one route to the generation of a metal is to allow filled and empty bands to overlap as in Figure 5 Elemental potassium is a metal because of a partially filled 4*s* band, a result which might suggest that elemental calcium, with a filled 4*s* band might be an insulator However, under ambient conditions calcium is a metal because filled 4*s* and empty 4*p* bands overlap Elemental nickel is analogously a metal because filled 3*d* and empty 4*s* bands overlap In both of these cases band overlap is also associated with mixing or hybridization between the levels concerned Elemental grey arsenic is a semi-metal due to overlap of valence and conduction bands *via* interactions between adjacent sheets in the solid Band overlap may be achieved by increasing the pressure on the solid Iodine, for example, forms a molecular solid but the levels have a non-zero width *via* the formation of energy bands since there are significant interactions between the orbitals on adjacent molecules As pressure is applied the band gap smoothly drops to zero (~ 170kbar) and at the same time the solid becomes metallic, and increasingly so as the band overlap increases (Figure 6) Sometimes the bands which overlap interact strongly with each other For example *s*–*p* mixing is so strong in diamond that a gap is generated[4] and an insulator results In graphite an analogous process occurs, but only with the in-plane *p* orbitals There can be no such interaction between 2*s* and 2*p*π orbitals by symmetry and the result is metallic graphite

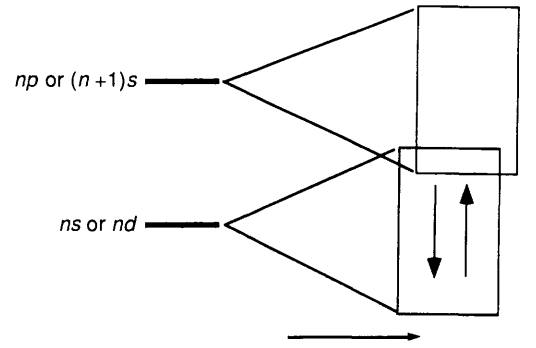

Figure 5 The generation of a metal by overlap of filled and empty bands Filled and empty bands are the *ns* and *np* respectively for the Group 2 elements and *nd* and $(n + 1)s$ for the Group 10 elements

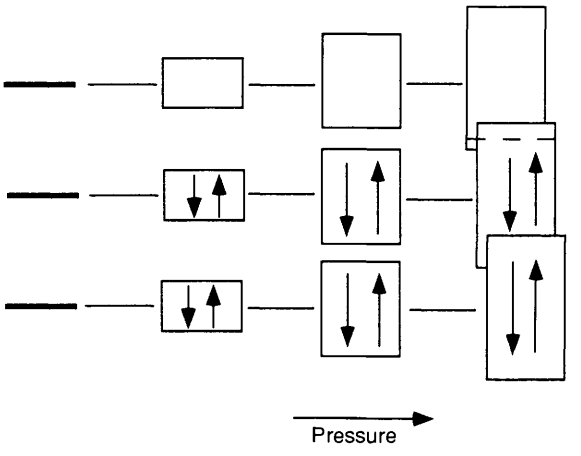

Figure 6 Broadening and eventual overlap of molecular levels as the intermolecular separation is decreased in iodine for example

The converse of the above is the generation of an insulator or semiconductor by removal of band overlap Although grey arsenic is metallic because of band overlap, the isoelectronic Zintl phases $Sr[Sn_2As_2]$, K[SnSb], and K[SnAs] are semiconductors They contain arsenic-like sheets[12] and the Group 14 and 15 atoms alternate in the structure All three are semiconductors in contrast to the behaviour of grey arsenic For $Sr[Sn_2As_2]$ the gap is smaller than in the other two compounds The reason is easy to see just by looking at the structure In the potassium-containing compounds these ions are arranged in layers which alternate with the SnAs or SnSb sheets and in the strontium-containing compound, these metal ions are only found between every other pair of sheets The potassium ion spacer in K[SnAs] and K[SnSb] increases the separation between the sheets, decreases the interaction between them, and removes the overlap of valence and conductor bands (the reverse of Figure 6*a*) The materials become semiconductors Because of the stoichiometry there is one set of non-bonded close contacts between adjacent SnAs sheets in $Sr[Sn_2As_2]$ which are absent in the potassium-containing compounds The semiconducting gap is thus smaller than in K[SnAs] and K[SnSb] In grey arsenic each sheet has close contacts on both sides The two examples that follow are much more subtle in an electronic sense

3.3 Metallic Behaviour of Supported Monolayers

A novel metal–insulator transition occurs in metal monolayers [13] Experiments in recent years have characterized the properties of monolayers of the late transition metals (M = Ni,

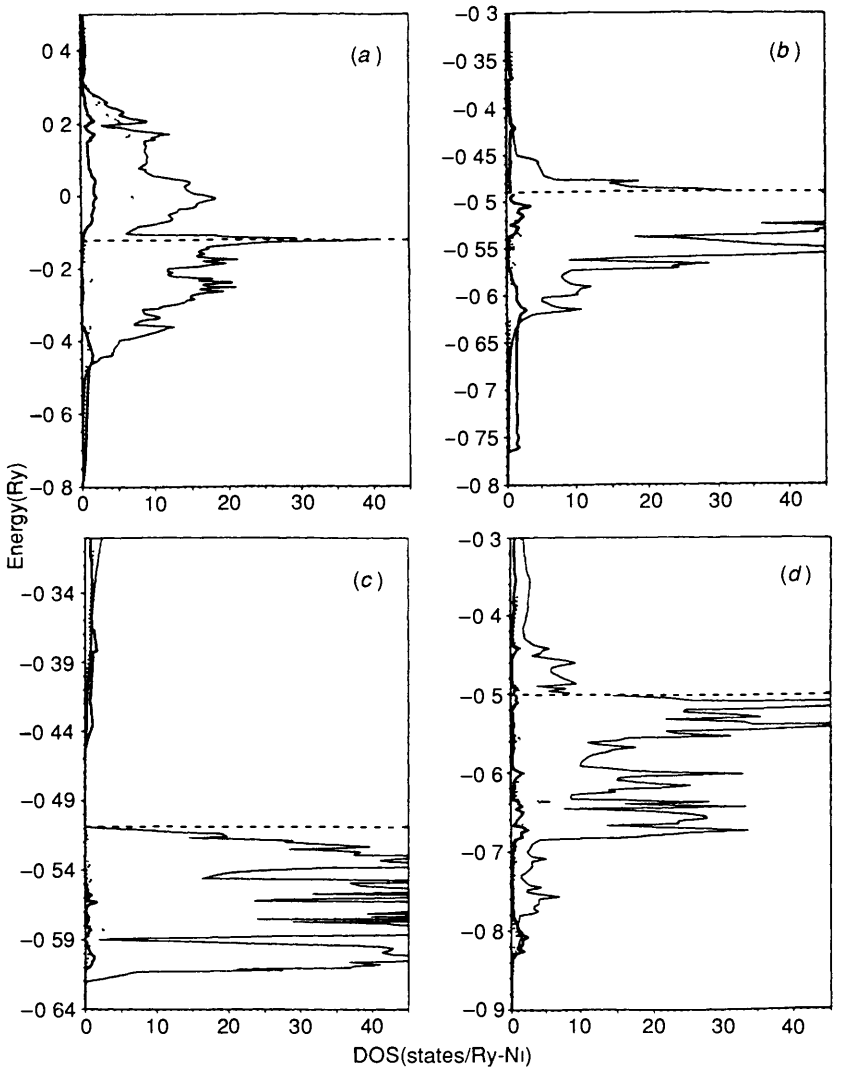

Figure 7 Computed electronic density of states for (a) bulk nickel, (b) a nickel monolayer, (c) a nickel monolayer on an oxide support, and (d) a two-atom thick multilayer of nickel on an oxide support

Pd, Ag, Hg, or Cu) supported on a 'cushion' of either X = H, O, or CO adsorbed on a W(110) surface, W(110)/X/M Interestingly W(110)/O/Ni does not behave metallically at all but W(110)/H/Ni does Thus the metallic properties of the overlayer metal M appear to be determined by the nature of the 'cushion', X This behaviour shows up clearly in electronic structure calculations carried out using the first principles LMTO approach [14] Figure 7 compares the computed electronic densities of states for bulk nickel and for a nickel monolayer Both are predicted to be metallic The band widths are smaller for the monolayer than for the bulk, a result of the smaller coordination number in the monolayer The *d–s* band overlap and hybridization, characteristic of the transition metals leads to approximately one ($s + p$) electron in the metallic structure of the sheet Thus the Fermi level for nickel lies below the top of the (largely) *d* band The situation is just as represented in Figure 5

However, the presence of the underlying support changes the picture completely for the Group 10 case We know from studies[5] on complexes of transition metal atoms with ligands of a variety of types that the metal ($n + 1$)*s* orbitals are destabilized much more strongly than the corresponding *nd* orbitals on ligand coordination An exactly analogous process is calculated to occur when the monolayer is 'coordinated' to the cushion material The ($n + 1$)*s* and *nd* bands are separated in energy (Figure 5*a*) and non-metallic behaviour results for the Ni sheet Now the Fermi level for nickel lies above the top of the (largely) *d* band Since the monolayer in proximity to the cushion leads to a gap but the bulk metal is an electronic conductor, the gap between *d* and *s* bands will disappear as the number of layers of the metal M increase, *n* in W(110)/X/M_n Figure 7 also shows the calculated density of states for the case of $n = 2$ where the gap has indeed closed Analogous considerations for copper show it is metallic under all of these conditions

3.4 The Metal–Almost Insulator Transition of Calcium under Pressure

We noted earlier that since the energy bands of solids broaden with a decrease in interatomic separation, a general prediction is that all materials should become metallic under pressure A different result at intermediate pressures is found for the Group 2 elements, Ca–Ba, and some of the lanthanide elements with the s^2 configuration Their conductivity decreases[11] with an increase in pressure and, in the case of Yb, a semiconductor is generated Such behaviour is not found for the Group 12 metals, zinc and cadmium, which have a d^{10} core However there is a structural distortion away from the *hcp* structure found for these elements which is connected to the rather unusual observation for the Group 2 elements

The experimental observations for the Group 2 elements are matched by band structure calculations which show that overlap of *s* and *p* bands of Figure 5 is almost completely removed as the

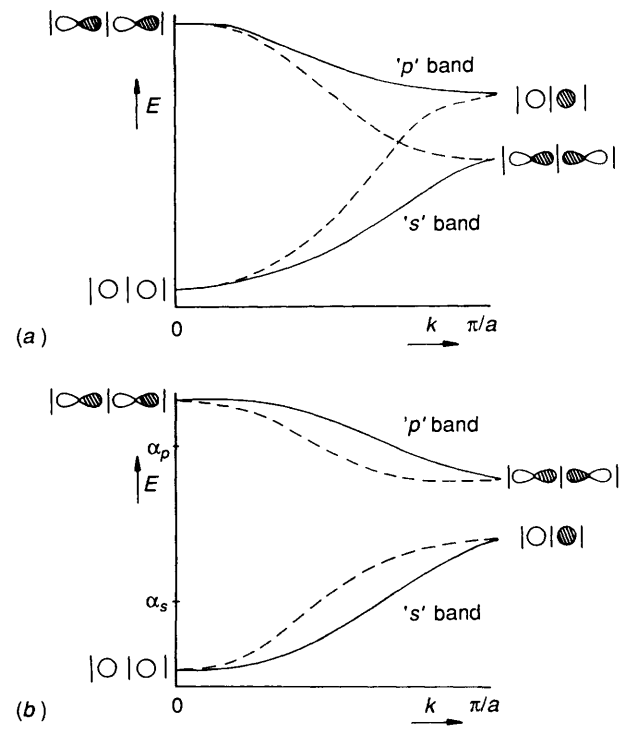

Figure 8 The *s* and *p* bands of a linear chain (a) where the *s p* separation is small compared to the inter orbital interactions and (b) where the converse is true

volume of the unit cell is reduced The result is the opposite to the 'usual' one of Figure 6 Although the three-dimensional band structure of the *fcc* solid is a non-trivial matter to derive, study of the orbital properties of a simple one-dimensional chain will be quite sufficient to understand what is behind this interesting result [15] Generation of the band structure of a linear atomic chain containing *s* and *pσ* orbitals requires solution of the relevant secular determinant which includes three different values of β, appropriate for *pσ–pσ*, *s–s* and *pσ–s* interactions It may be readily written down as

$$\begin{vmatrix} \alpha + 2\beta_{ss}\cos ka - E & 2i\beta_p \sin ka \\ -2i\beta_p \sin ka & \alpha_p - 2\beta_{pp}\cos ka - E \end{vmatrix} = 0 \qquad (5)$$

The algebraic solution will not be derived explicitly but there are important symmetry restrictions which control the form of the wavefunctions At the points Γ (0 $(2\pi/a)$) and X ($\frac{1}{2}$ $(2\pi/a)$) the group of $\boldsymbol{k}$ contains the elements $\{E, \imath\}$ but for any other $\boldsymbol{k}$ the group contains $\{E\}$ only The group of order two which contains $\{E, \imath\}$ contains two different symmetry species, one symmetric (Γ_1) and one antisymmetric (Γ_2) with respect to inversion The group of G, the general point, which contains $\{E\}$ alone, only contains a single irreducible representation (G_1) Thus at the symmetry points, Γ and X, the *s* and *pσ* orbitals transform as $\Gamma_1 + \Gamma_2$ (or $X_1 + X_2$) but as $2G_1$ at general points in between This important result, seen algebraically in equation 5 too, is that *s–p* mixing only occurs at general points in the Brillouin zone (and is a maximum for $k = \pi/2a$) At both zone centre and zone edge the crystal orbitals are either pure *s* or pure *p* in character Two different types of behaviour are thus forced by this last statement and are shown in Figure 8 If the *s–p* separation is large compared with the values of β for the *s* and *p* bands then two bands each bounded by the energy of the relevant in-phase and out-of-phase orbital combinations are found (Figure 8a) Mixing between *s* and *p* orbitals at general $\boldsymbol{k}$ points occur and is shown by the dashed lines Figure 8b shows the case where the unmixed *s* and *p* bands (dashed lines) cross in energy, in other words the in-phase *pσ* combination lies deeper in energy than the out-of-phase *s* orbital combination Importantly, note that the lower energy band, the '*s*-band, while purely *s–s* bonding at the zone centre, is purely *p p* bonding at the zone edge

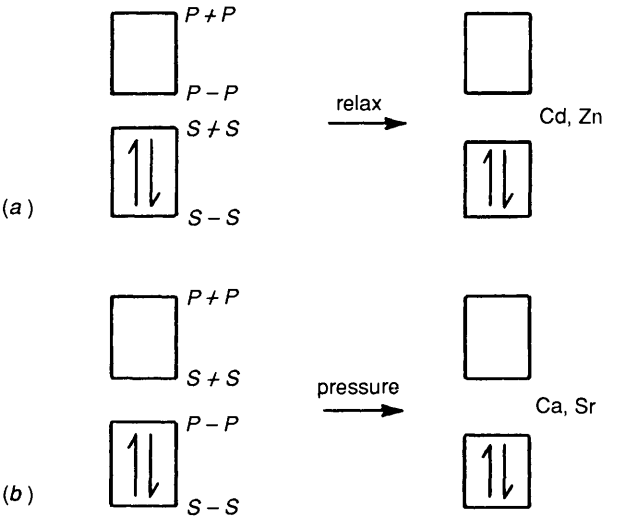

Figure 9 Expected behaviour of the electronic situations of Figure 8 under pressure

Extension of this discussion to three dimensions leads to an understanding (Figure 9) of the behaviour under pressure of the s^2 and $d^{10}s^2$ metals Whether case (a) or (b) is found depends upon the values of α_s, α_p, and β_{ij} Larger values of β_{ij} usually correspond to shorter interatomic separations In fact elemental zinc corresponds to case (a) but elemental calcium to case (b) For the former the electronic situation is a little like that for He_2 Bringing together two filled *s* bands should lead overall to a repulsion between the atoms An increase in metal–metal distance along *c* is the result found for zinc and cadmium Both elements crystallize in the *hcp* structure, but with *c/a* ratios (1 856, 1 886 respectively) quite different from the ideal value of 1 633 Thus the structure is stretched along the *c* direction An increase in pressure leads to broadening of both bands just as in Figure 6

By way of contrast, a reduction in the internuclear separation, occurring with an increase in applied pressure, should have very different effects on the relative energies of the top of the lower band and bottom of the upper band of Figure 9a Since bonding levels should drop in energy and antibonding ones should rise in energy, the *s–p* gap should increase This is the case for calcium, and as the metal–metal distance becomes smaller the gap between the two bands increases, as shown by the full band structure of the material [15]

3.5 Band Gap in d^6 Perovskites

Molecular transition metal complexes have a gap between the *d* orbitals of e_g and t_{2g} type which is determined in textbook fashion by the σ and π strength of the coordinated ligands It is interesting to see how the size of the band gap between the *d* bands of e_g and t_{2g} type in some solids is determined by somewhat more complex orbital considerations [16] The size of the gap determines properties of the solid of course The perovskite $LaRhO_3$ is non-metallic with a gap of ~ 1 6 eV but although the isoelectronic $LaCoO_3$ with the same structure is also non-metallic, it is only just so The gap is small, so that at higher temperatures a whole series of transformations take place triggered by thermal excitation of electrons from valence to conduction band Thus the chemical identity of the system is vital here

Since the BO_3 part of the ABO_3 perovskite structure is composed of three identical, mutually perpendicular O–M–O–M–O chains the essence of the electronic arguments will be contained in the band structure of just one of these

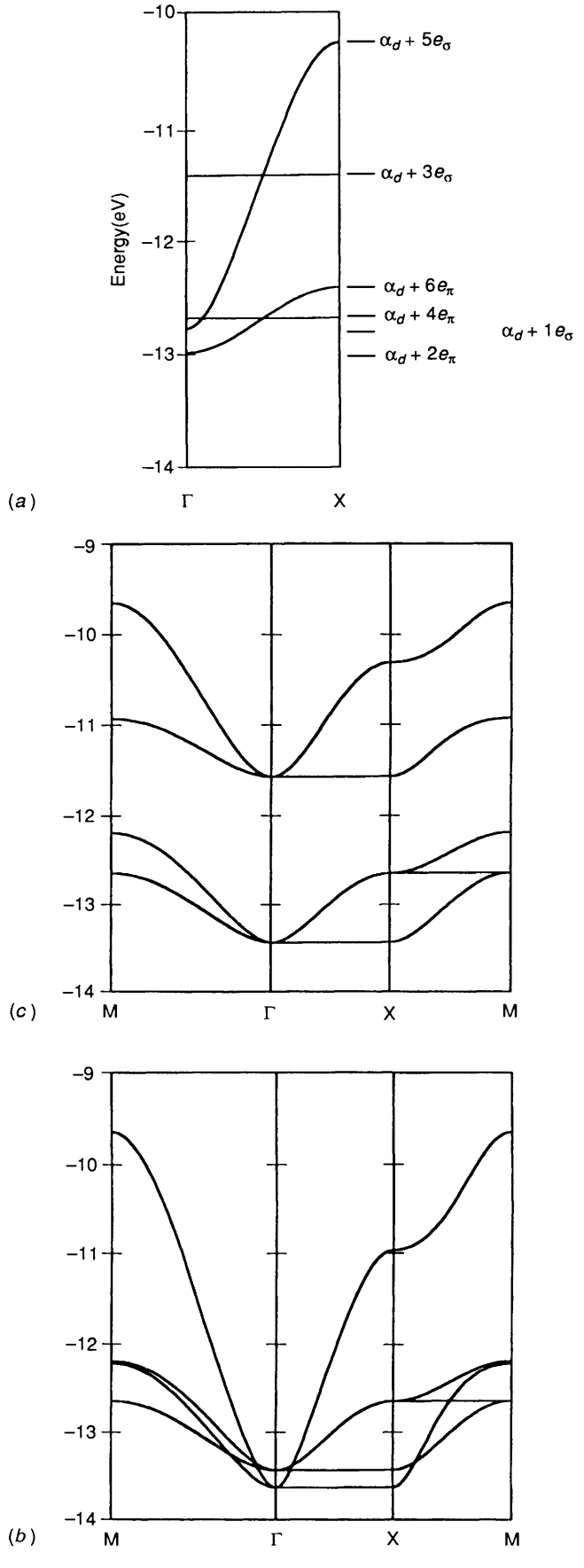

Figure 10 (a) Dispersion behaviour of the bands of a one-dimensional perovskite chain The σ and π bands overlap (Energies shown are from the angular overlap model) (b) The d bands *via* metal d oxygen $p\sigma$ orbital interactions in a square MO_2 net (Figure 11b) (c) The same as (b) but including metal d oxygen s orbital interactions

units As in the molecule, by symmetry there is no mixing between the σ (e_g) or π (t_{2g}) bands, It will be useful to take advantage of some further symmetry arguments As argued above for the simple sp chain at the points Γ (0 ($2\pi/a$)) and X ($\frac{1}{2}$ ($2\pi/a$)) the group of $\boldsymbol{k}$ contains the elements $\{E, i\}$, but for any other $\boldsymbol{k}$ the group contains $\{E\}$ only Also at the zone centre the wavefunction must be symmetric from cell to cell, and at the zone edge antisymmetric This means that on a p-orbital-only model (Figure 10a) there can be no $p\sigma$ or $p\pi$ contribution at the bottom of either the $p\sigma$ (e_g) band which lies at Γ or $p\pi$ (t_{2g}) band which lies at X The bottom of both bands thus lie at the unperturbed d orbital energy The energies depicted come from the angular overlap model On this model there is no gap at all between the d bands of e_g and t_{2g} type, and thus all d^n perovskites ($0 < n < 10$) including those with the d^6 configuration should be metals The same results applies to the two-dimensional net (Figure 10b) Inclusion of oxygen s orbitals changes the picture (Figure 10c) Whereas interaction of oxygen p with metal d is zero at Γ and non-zero at X, the converse is true for interaction of oxygen s with metal d because of the difference in orbital parity Thus it is inclusion of oxygen s/metal d interactions which open the e_g/t_{2g} gap in the perovskites The magnitude of the gap is thus not solely determined by the balance between σ and π donor effects as in molecules, but by the differential effects of metal–oxygen $s\sigma$ and metal–oxygen $p\sigma$ interactions Thus prediction of the magnitude of the gap without a calculation is extremely difficult Unlike the case of the Zintl compounds, where electronic saturation usually leads to semiconducting behaviour, the e_g/t_{2g} gap in transition metal systems is frequently non-existent and the state of affairs system-dependent

4 High-temperature Superconductors

4.1 The Importance of Two-electron Terms

Perhaps the classic cases of control of metallic or insulating properties by the balance of one- and two-electron terms in the energy come from the area[1] of doped transition metal oxides This is especially important for oxides containing first-row metals The recently-discovered group of high-temperature superconducting oxides based on doped cuprates are particularly interesting examples Identification of the nature of the superconducting state has proved elusive (however, see reference 17), but the geometrical control of the electronic structure and ultimately therefore the superconducting properties of these materials are striking

Three examples from the series of the superconducting cuprates will be discussed in this section As in all materials of this type they contain[18] sheets of stoichiometry CuO_2 (Figure 11) $La_{2-x}Sr_xCuO_4$, one of the very first 'high-temperature' superconductors with a T_c of 35 K for $x \sim 0.15$ contains distorted CuO_6 octahedra vertex-fused in two dimensions (Three-dimensional vertex fusion leads to the perovskite structure and thus to the frequently used description of this family of compounds as 'perovskite superconductors') Jahn–Teller distortions are typical of Cu^{II} and here two long axial and four short equatorial Cu–O distances are found The La (and Sr) atoms lie between these sheets Since these axial Cu–O distances

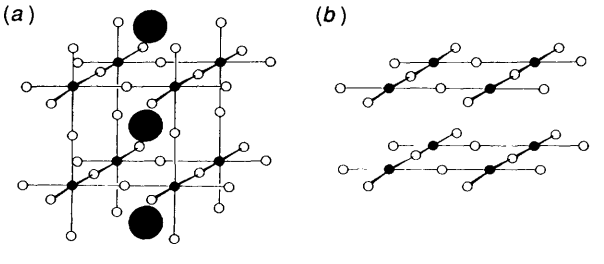

Figure 11 (a) The perovskite structure (b) A sheet of stoichiometry CuO_2 found in all cuprate superconductors Often the sheet is not planar being slightly puckered or rumpled

are long ones, a good way of describing the solid is as alternating layers of rocksalt (La,Sr)O and perovskite CuO_2 layers In superconductors containing bismuth and thallium, Bi_2O_2 and Tl_2O_2 rocksalt layers are found here too The first 'high-temperature' superconductor to be discovered with a T_c above liquid nitrogen temperature, was $YBa_2Cu_3O_7$,[18] with a T_c of ~ 95 K Figure 12 shows the structure of the compound There is a range of oxygen stoichiometry possible in the inter-planar region, namely $YBa_2Cu_3O_{7-\delta}$, $0 < \delta < 1$ and an interesting dependence of T_c on δ There is a precipitous drop at around $\delta = 0.65$ where the compound becomes an antiferromagnetic insulator The parent compound $YBa_2Cu_3O_7$ (Figure 12) contains two types of copper atom, square pyramidal Cu(1) and square planar Cu(2) Since the fifth Cu(1)–O distance is quite long, a good description of the structure is of chains of copper, Cu(2), in square planar coordination sandwiched between planes of copper, Cu(1) As oxygen atoms are lost from the chains with an increase in δ, linear two-coordinate copper atoms are generated so that in $YBa_2Cu_3O_6$ all of the inter-planar copper atoms are two coordinate Many superconducting cuprates are now known, and all may be described geometrically as containing sheets of CuO_2 stoichiometry (where superconduction occurs) alternating with sheets or slabs of insulating material The latter, described as 'reservoir' material for reasons which will become apparent below, constitute a spatially distinct region separated from the CuO_2 sheets by the long axial Cu–O distances in the octahedra The formulae of the systems described above may then be rewritten as $(La_{2-x}Sr_xO_2)(CuO_2)$ and $(Y)(Ba_2CuO_3)(CuO_2)_2$ to highlight this geometrical (and electronic) simplification In the former the reservoir material is a slab of rocksalt-like $La_{2-x}Sr_xO_2$ and in the latter there are two types of reservoir material (Figure 12), namely layers of Y atoms and the CuO_3 chains of square planar Cu(2) linked by Ba atoms In superconductors containing bismuth and thallium, $(BiO)_2$ and $(TlO)_2$ rocksalt layers are found $Tl_2Ba_2Ca_{n-1}Cu_nO_{2n+4}$, written as $(Tl_2O_2)(Ba_2O_2)(Ca_{n-1})((CuO_2)_n)$ contains distorted Tl_2O_2 double rocksalt layers between the CuO_2 sheets, whereas $TlBa_2Ca_{n-1}Cu_nO_{2n+3}$ contains single TlO layers, $(TlO)(Ba_2O_2)(Ca_{n-1})((CuO_2)_n)$

Although some of these systems are formally electron-doped compounds (*e g* , $Nd_{2-x}Ce_xCuO_4$) the majority are hole-doped (*e g* , $La_{2-x}Sr_xCuO_4$) The compositional dependence of the properties of this second group appear to be reasonably similar As shown in the generic diagram[18] of Figure 13 the materials may be converted from an antiferromagnetic insulator into a superconducting metal and then into a normal metal *via* a change in copper oxidation state Specifically for $La_{2-x}Sr_x$-CuO_4, T_c reaches a maximum at $x \sim 0.15$ where the change in copper oxidation state is controlled by substitution of a two-valent ion for a three-valent one (*e g* , Sr for La) The presence of defects (non-stoichiometric amounts of oxygen or bismuth or thallium for example) are effective in this regard too in many of the bismuth- or thallium-containing superconductors The reservoir material composition and structure determines the oxidation state of the copper atoms in the CuO_2 planes There are considerable experimental problems in determining the exact stoichiometry in many of these systems

The construction of a band picture for the CuO_2 sheet for the region where the molecular orbital, Mulliken–Hund approach, is valid is straightforward The *d* orbital level splitting pattern expected for a planar CuO_4 fragment and the band generated for the extended CuO_2 array is shown in Figure 14 Since the axial Cu–O distances are long the z^2 orbital lies at low energy, stabilized in this geometry too by *d–s* mixing The $x^2 - y^2$ orbital of the metal, the highest occupied orbital of the fragment is involved in σ interactions with the ligands Since the atomic energies of the copper 3*d* and oxygen 2*p* orbitals are similar, strong mixing between them is to be expected This level, occupied by the single unpaired electron of Cu^{II}, is antibonding between copper and oxygen,[2] a result which shows up experimentally as a strong dependence of Cu–O distance on doping The band is metal–oxygen antibonding and thus addition of

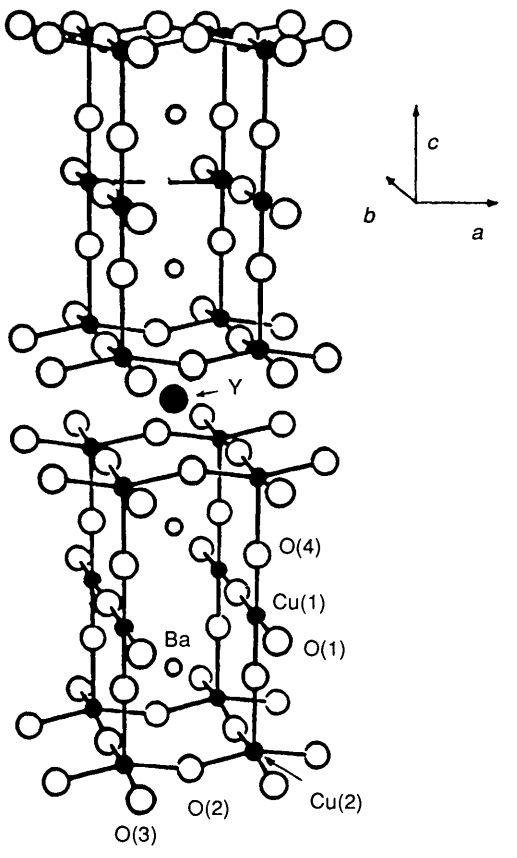

Figure 12 The structure of $YBa_2Cu_3O_{7-\delta}$

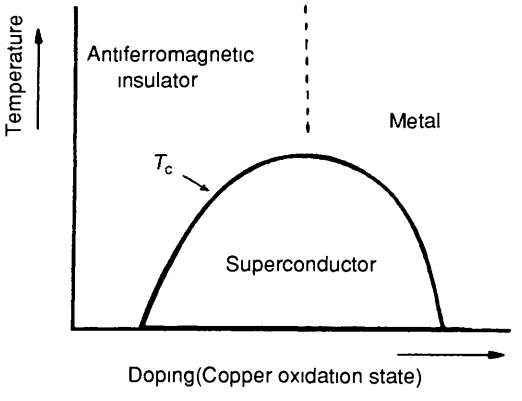

Figure 13 A generic picture showing how the antiferromagnetic insulating state for a cuprate may be doped to give a metal and superconductor

electrons (as in $Nd_{2-x}Ce_xCuO_4$) should lengthen, and removal of electrons (as in $La_{2-x}Sr_xCuO_4$) should shorten the Cu–O distance By and large this is true, but the steric demands of the reservoir material also influence these distances

The result for La_2CuO_4 itself is a half-filled band situation Since the on-site Coulomb repulsion, *U*, for this first row metal (Cu) is expected to be large, κ will be large too and an antiferromagnetic insulator should be favoured This is what is found experimentally for the undoped material Addition of holes probably leads initially to the generation of small polarons (*vide supra*) which eventually collapse to give a metal at a critical doping level Addition of these holes suppresses the CDW instability expected for the half-filled metallic band, and so on doping a metal is eventually generated It happens to be a superconductor too It is interesting to ask how important is the rôle played by copper in these systems For this we turn to some

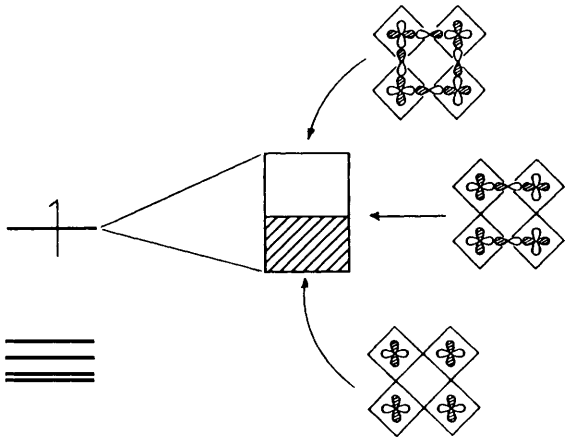

Figure 14 Simple derivation of the band structure of a sheet of stoichiometry CuO_2

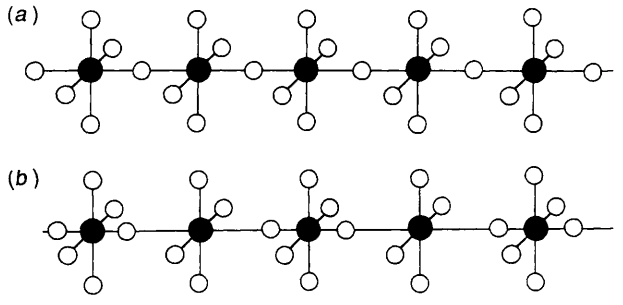

Figure 15 (a) Symmetrical and (b) distorted structures for platinum and nickel mixed-valence chains

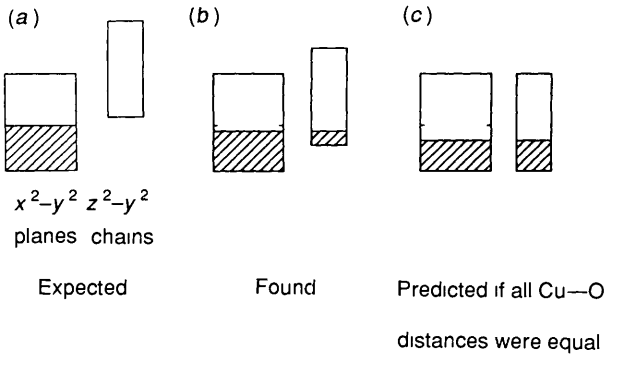

Figure 16 Band overlap in $YBa_2Cu_3O_{7-\delta}$ (a) None leading to no plane chain charge transfer (b) the actual state of affairs (c) overlap expected if the plane and chain Cu–O distances are equal

interesting results concerning the one-dimensional analogues of these CuO_2 sheets, namely the platinum mixed-valence compounds, and their nickel analogues (Figure 15) Here the highest occupied band is the 'z^2' band of the chain The oxidation state of the platinum in the symmetrical structure in Figure 15a is Pt^{III} and thus this 'z^2' band is half-full of electrons A Peierls distortion is expected and indeed the symmetric system Figure 15a distorts to Figure 15b The initially metallic state has become insulating, although as in the case of elemental iodine and phosphorus the conductivity of these salts increases markedly with application of pressure Some of the nickel analogues are found as antiferromagnetic insulators with an undistorted structure This behaviour is very similar to that found for molecular complexes of nickel and platinum and readily understood from Jahn–Teller considerations The singlet–triplet splittings for the first-row nickel atom are larger than for its third-row congener, and the magnitude of the orbital interactions are larger for platinum than for nickel The result is thus always diamagnetic square-planar complexes for Pt^{II} (*e g* , $Pt(CN)_4^{2-}$) but the frequent observation of high-spin octahedral complexes for Ni^{II} (*e g* , $Ni(H_2O)_6^{2+}$) The important parameter in the molecular case is again the critical ratio of these one-electron (Jahn–Teller stabilization energy) to two-electron (singlet–triplet splitting) energy terms From this viewpoint one would suspect that silver analogues of the cuprate superconductors would be susceptible to strong Peierls distortions which would destroy the metallic AgO_2 sheet Indeed no silver compounds structurally analogous to these cuprates are known

4.2 Band Overlap and the Generation of a Metallic State

It was a straightforward matter to determine the copper oxidation state in $La_{2-x}Sr_xCuO_4$ but how the oxidation state of the planar copper atoms depend on oxygen stoichiometry in $YBa_2Cu_3O_{7-\delta}$, is a more complex question [2] Square planar coordination is found for both Cu^{II} and Cu^{III}, and square pyramidal geometries, always with long apical bonds, only for Cu^{II} Such observations indicate that the formula $YBa_2(Cu^{II}O_2)_2(Cu^{III}O_3)$ should be a correct description of the compound with $\delta = 0$ Similarly, $YBa_2(Cu^{II}O_2)_2(Cu^{I}O_2)$ should be a good way to describe the compound with $\delta = 1$ Linear two-coordination is a common geometry for Cu^{I} Both pictures lead to a formal oxidation state of Cu^{II} for the copper atoms in the superconducting planes and do not answer the question of why $YBa_2Cu_3O_7$ is a metal but $YBa_2Cu_3O_6$ an antiferromagnetic insulator Both compounds on the simplest model with a half-filled $x^2 - y^2$ band should behave like La_2CuO_4 and be insulators It is vital to examine the form of the band structure of the material[2] to see how the CuO_2 planes for $\delta = 0$ are doped away from the half-filled band and thus described by the generic picture of Figure 13

The details of the band structure of the material are both simple and interesting Since there are now two different types of square-planar copper there will be two types of $x^2 - y^2$ bands Both may be constructed in the same fashion as shown in Figure 14 (The z^2 orbital may be ignored since it lies deep in energy) Since the $x^2 - y^2$ band associated with the planes is of δ symmetry with respect to the inter-planar material it is uncoupled from the energy bands of the chains since there are no oxygen orbitals of that symmetry The $x^2 - y^2$ band for the chains needs to be relabelled as $z^2 - y^2$ since the chains run in the yz plane The electronic description of $YBa_2Cu_3O_7$ depends crucially on the relative locations of these two sets of bands the $x^2 - y^2$ band of the CuO_2 planes and the $z^2 - y^2$ band of the CuO_3 chains Writing the $\delta = 1$ system as $YBa_2(Cu^{II}O_2)_2(Cu^{III}O_3)$ forces the description of Figure 16a where the chain $z^2 - y^2$ band is empty and thus Cu(2) described formally as Cu^{III}, and the plane $x^2 - y^2$ band is half full so that Cu(1) is described as Cu^{II} (The different numbers of copper atoms of the two types, Cu(1,2) are indicated by drawing the boxes of different width) The true situation is somewhat different since the two bands overlap (Figure 16b) so that the electron transfer occurs from planes to chains The half-filled band is avoided for the Cu(1) atoms of the CuO_2 planes and a metal may result In electronic terms the interplanar CuO_3 unit plays therefore the same rôle as substitution of Sr for La in the La_2CuO_4 system The details of the local copper coordination geometry control the band overlap and hence charge transfer If the square-planar bond lengths and the in-plane square-pyramidal bond lengths were equal, the $x^2 - y^2$ and $z^2 - y^2$ bands, while being of different widths would be similarly energetically located as in Figure 16c Their overlap would lead to around 0 33 holes on each planar copper atom Since the bond lengths in the planes (average 1 944 Å) are substantially longer than those in the chains (average 1 888 Å) the result is destabilization of the $z^2 - y^2$ band relative to $x^2 - y^2$, but maintaining overlap between them (Figure 16b) such that charge transfer may occur between the two The same model allows access to the behaviour

of $YBa_2Cu_3O_6$ Here there is no chain $z^2 - y^2$ band which may overlap with $x^2 - y^2$ and the planar copper oxidation state is that given by the formula $YBa_2(Cu^{II}O_2)_2(Cu^{I}O_2)$ Now the electronic state of affairs with a half-filled band is similar to that of undoped La_2CuO_4 and an antiferromagnetic insulator results In these cuprate superconductors there are thus two distinct ways to remove electron density from the planar $x^2 - y^2$ band, by doping and by band overlap As oxygen is removed from between the sheets the extent of plane-chain doping gradually decreases (Figure 17), and somewhere corresponding to a stoichiometry between $YBa_2Cu_3O_{6.5}$ and $YBa_2Cu_3O_6$ a metal–insulator transition is to be expected This shows up in the T_c dependence plot on δ where the superconducting temperature drops precipitously to zero as the insulator is generated There are also structural changes in the material which show up most in changes in the c-axis of the material

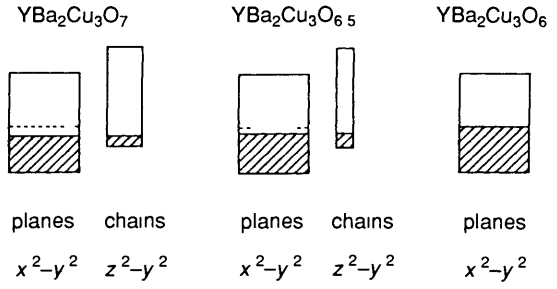

Figure 17 Chain plane electron transfer in $YBa_2Cu_3O_7$ and $YBa_2Cu_3O_{6.5}$ and its absence in $YBa_2Cu_3O_6$

Band overlap controls the properties of other superconductors too Overlap is found to occur by calculation[19] in $Tl_2Ba_2Ca_{n-1}Cu_nO_{2n+4}$, which as noted above contains distorted Tl_2O_2 double rocksalt layers between the CuO_2 sheets There is however no computed overlap in the material $TlBa_2Ca_{n-1}Cu_nO_{2n+3}$ which contains single TlO layers There is a simple electronic explanation for the difference between the two Just as the 'band width' of a simple polyene increases as the number of atoms increases (asymptotically approaching the value found for the infinite system), so the contribution to the band width of the Tl_nCl_n unit increases with the number of atoms or units (n) in the direction perpendicular to the slab Thus the Tl_2O_2 bandwidth is larger than that for the single TlO layer (Figure 18a, b) Another pair of systems where metallic (and superconducting) behaviour is simply controlled by hand overlap is $TlMRECuO_5$ Superconductors are found for RE = La, Nd and M = Sr, but not for its M = Ba analogues, even though the two systems are isostructural There is though a small difference between the cell parameters of the Sr and Ba analogues resulting in a small difference in the Cu–O bond lengths in the two materials [The crystallographic a parameters (roughly twice the Cu–O distance) are 3 849 Å (Ba) and 3 761 Å (Sr)] This difference of about 0 05 Å in the Cu–O distance is sufficient to raise the energy of the $x^2 - y^2$ band of the CuO_2 sheet so that band overlap with the TlO layer may occur in the Sr case but not for Ba, as shown qualitatively in Figure 18c, d

These doping models are applicable[2] to all of the presently known high-T_c superconductors The band model predicts a half-filled $x^2 - y^2$ band for Cu^{2+}, an electronic configuration susceptible to two types of instability which lead to the creation of an insulator Both localization *via* a large on-site Coulomb repulsion or a Peierls distortion are routes away from the metallic state Electrons need to be added or removed from this band to generate a metal Some of the high-temperature superconductors appear to be electron doped but the majority are hole-doped, where electrons are removed from the half-full band There are two routes to this state of affairs, either by overlap with an empty band or a change in stoichiometry Although the second mechanism is easily understandable by consideration of the chemical formula, *via* cation substitution,

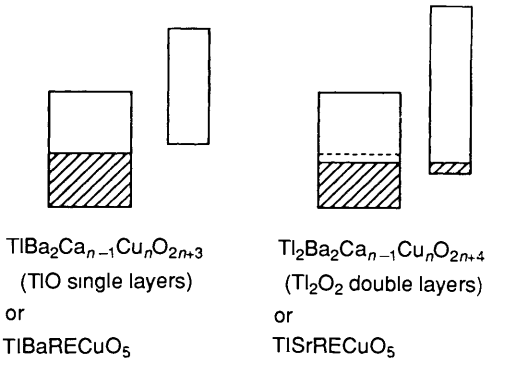

Figure 18 Band overlap in $Tl_2Ba_2Ca_{n-1}Cu_nO_{2n+4}$ which contains single Tl_2O_2 double rocksalt layers between the CuO_2 sheets, but no band overlap in $TlBa_2Ca_{n-1}Cu_nO_{2n+3}$ which contains single TlO layers Similar results apply to $TlMRECuO_5$ where M = Sr and Ba respectively

cation vacancies, or the presence of extra oxygen, the first requires a detailed understanding of the electronic structure In some materials certainly both mechanisms are at work

5 Epilogue

It should be apparent from the discussion in this review that *a priori* prediction of metallic or insulating properties is not straightforward Some of the stoichiometry or structural changes involved are very small indeed For example, substitution of only 4% of the lanthanum by strontium in La_2CuO_4 is sufficient to convert an insulator into a metal, and a superconductor at that Similarly, the difference in cell constant between $TlBaRECuO_5$ (an insulator) and $TlSrRECuO_5$ (a superconductor) is small The difference in the orbital interactions between metal and oxygen s and p orbitals which controls the band gap in d^0 perovskites is a parameter difficult to easily assess in qualitative terms The rôle of the structure itself is an important one and varies from the obvious (*e g* , diamond and graphite) to the subtle (*e g* , the doping mechanism in $YBa_2Cu_3O_7$)

6 References

1 (*a*) J B Goodenough, 'Magnetism and The Chemical Bond', Wiley, 1963, (*b*) J B Goodenough, *Prog Solid State Chem* , 1971, **5**, 143, (*c*) P A Cox, 'The Electronic Structure and Chemistry of Solids', Oxford, 1987
2 J K Burdett, in ref 18(*a*)
3 (*a*) M J S Dewar, 'Theory of Molecular Orbitals', McGraw-Hill, 1969, (*b*) A Haug, 'Theoretical Solid State Physics', Pergamon Press, 1972
4 J K Burdett, 'Chemical Bonding in Solids', Oxford, 1994
5 T A Albright, J K Burdett and M -H Whangbo, 'Orbital Interactions in Chemistry', Wiley, 1985
6 E Canadell and M -H Whangbo, *Chem Rev* , 1991, **91**, 965
7 J K Burdett and S Lee, *J Am Chem Soc* 1983, **105**, 1079
8 L C Allen, *J Am Chem Soc* , 1992, **114**, 1510
9 W P Anderson, J K Burdett, and P T Czech, *J Am Chem Soc* , 1994, **116**, 8808
10 K A Y Yee and T Hughbanks, *Inorg Chem* , 1991, **30**, 2321
11 N F Mott, 'Metal–Insulator Transitions', Taylor and Francis, 1974
12 P C Schmidt, D Stahl, B Eisenmann, R Kneip, V Eyert, and J Kubler, *J Solid State Chem* , 1992, **97**, 93
13 N Shamir, J C Lin, and R Gomer, *J Chem Phys* , 1989, **90**, 5135, J E Whitten and R Gomer, *Surface Science*, 1994, **316**, 36
14 J K Burdett and S Sevov, *J Chem Phys* , 1994, **101**, 840
15 T L Brennan and J K Burdett, *Inorg Chem* , 1993, **32**, 750
16 J K Burdett and S A Gramsch, *Inorg Chem* , 1994, **33**, 4309
17 J K Burdett, *Inorg Chem* , 1993, **32**, 3915
18 (*a*) 'Chemistry of High-Temperature Superconductors', ed T A Vanderah, Noyes, 1991, (*b*) J K Burdett, *Adv Chem Phys* , 1993, **83**, 207
19 D Jung, M -H Whangbo, N Herron, and C C Torardi, *Physica*, 1989, **C160**, 381